EUROPEAN ORGANIZATION FOR NUCLEAR RESEARCH

CERN-PPE/91-207

19 November 1991

Production of Strange Particles in the Hadronic Decays of the Z^0

DELPHI Collaboration

Abstract

An analysis of the production of strange particles from the decays of the Z^0 boson into multihadronic final states is presented. The analysis is based on about 90,000 selected hadronic Z^0 decays collected by the DELPHI detector at LEP in 1990. K^0_S, $K^{*\pm}$, $\Lambda(\overline{\Lambda})$ and $\Xi^-(\overline{\Xi}^+)$ have been identified by their characteristic decays. The measured production cross sections are compared with predictions of the Lund Monte Carlo tuned to data at PEP/PETRA energies.

(Submitted to Physics Letters B)

P.Abreu[18], W.Adam[43], F.Adami[34], T.Adye[32], T.Akesson[21], G.D.Alekseev[13], P.Allen[42], S.Almehed[21], S.J.Alvsvaag[4], U.Amaldi[7], E.Anassontzis[3], P.Antilogus[22], W-D.Apel[14], R.J.Apsimon[32], B.Åsman[38], J-E.Augustin[16], A.Augustinus[27], P.Baillon[7], P.Bambade[16], F.Barao[18], R.Barate[11], G.Barbiellini[40], D.Y.Bardin[13], A.Baroncelli[35], O.Barring[21], W.Bartl[43], M.J.Bates[30], M.Battaglia[25], M.Baubillier[20], K-H.Becks[45], C.J.Beeston[30], M.Begalli[10], P.Beilliere[6], Yu.Belokopytov[37], P.Beltran[9], D.Benedic[8], J.M.Benlloch[42], M.Berggren[16], D.Bertrand[2], F.Bianchi[39], M.S.Bilenky[13], P.Billoir[20], J.Bjarne[21], D.Bloch[8], S.Blyth[30], V.Bocci[33], P.N.Bogolubov[13], T.Bolognese[34], M.Bonapart[27], M.Bonesini[25], W.Bonivento[25], P.S.L.Booth[19], P.Borgeaud[34], G.Borisov[37], H.Borner[7], C.Bosio[35], B.Bostjancic[7], O.Botner[41], B.Bouquet[16], C.Bourdarios[16], M.Bozzo[10], S.Braibant[2], P.Branchini[35], K.D.Brand[31], R.A.Brenner[12], H.Briand[20], C.Bricman[2], R.C.A.Brown[7], N.Brummer[27], J-M.Brunet[6], L.Bugge[29], T.Buran[29], H.Burmeister[7], J.A.M.A.Buytaert[7], M.Caccia[7], M.Calvi[25], A.J.Camacho Rozas[36], A.Campion[19], T.Camporesi[7], V.Canale[33], F.Cao[2], F.Carena[7], L.Carroll[19], C.Caso[10], E.Castelli[40], M.V.Castillo Gimenez[42], A.Cattai[7], F.R.Cavallo[5], L.Cerrito[33], A.Chan[1], M.Chapkin[37], P.Charpentier[7], L.Chaussard[16], J.Chauveau[20], P.Checchia[31], G.A.Chelkov[13], L.Chevalier[34], P.Chliapnikov[37], V.Chorowicz[20], R.Cirio[39], M.P.Clara[39], P.Collins[30], J.L.Contreras[23], R.Contri[10], G.Cosme[16], F.Couchot[16], H.B.Crawley[1], D.Crennell[32], G.Crosetti[10], M.Croson[6], J.Cuevas Maestro[36], S.Czellar[12], S.Dagoret[16], E.Dahl-Jensen[26], B.Dalmagne[16], M.Dam[29], G.Damgaard[26], G.Darbo[10], E.Daubie[2], P.D.Dauncey[30], M.Davenport[7], P.David[20], W.Da Silva[20], C.Defoix[6], D.Delikaris[7], S.Delorme[7], P.Delpierre[6], N.Demaria[39], A.De Angelis[40], M.De Beer[34], H.De Boeck[2], W.De Boer[14], C.De Clercq[2], M.D.M.De Fez Laso[42], N.De Groot[27], C.De La Vaissiere[20], B.De Lotto[40], A.De Min[25], H.Dijkstra[7], L.Di Ciaccio[33], F.Djama[8], J.Dolbeau[6], O.Doll[45], M.Donsselmann[27], K.Doroba[44], M.Dracos[7], J.Drees[45], M.Dris[28], Y.Dufour[6], W.Dulinski[8], L-O.Eek[41], P.A.-M.Eerola[7], T.Ekelof[41], G.Ekspong[38], A.Elliot Peisert[31], J-P.Engel[8], V.Falaleev[37], D.Fassouliotis[28], M.Feindt[7], M.Fernandez Alonso[36], A.Ferrer[42], T.A.Filippas[28], A.Firestone[1], H.Foeth[7], E.Fokitis[28], P.Folegati[40], F.Fontanelli[10], K.A.J.Forbes[19], H.Forsbach[45], B.Franek[32], P.Frenkiel[6], D.C.Fries[14], A.G.Frodesen[4], R.Fruhwirth[43], F.Fulda-Quenzer[16], K.Furnival[19], H.Furstenau[14], J.Fuster[7], G.Galeazzi[31], D.Gamba[39], C.Garcia[42], J.Garcia[36], C.Gaspar[7], U.Gasparini[31], P.Gavillet[7], E.N.Gazis[28], J-P.Gerber[8], P.Giacomelli[7], K-W.Glitza[45], R.Gokieli[7], V.M.Golovatyuk[13], J.J.Gomez Y Cadenas[7], A.Goobar[38], G.Gopal[32], M.Gorski[44], V.Gracco[10], A.Grant[7], F.Grard[2], E.Graziani[35], G.Grosdidier[16], E.Gross[7], P.Grosse-Wiesmann[7], B.Grossetete[20], J.Guy[32], F.Hahn[7], M.Hahn[14], S.Haider[27], Z.Hajduk[15], A.Hakansson[21], A.Hallgren[41], K.Hamacher[45], G.Hamel De Monchenault[34], F.J.Harris[30], B.W.Heck[7], T.Henkes[7], I.Herbst[45], J.J.Hernandez[42], P.Herquet[2], H.Herr[7], I.Hietanen[12], C.O.Higgins[19], E.Higon[42], H.J.Hilke[7], S.D.Hodgson[30], T.Hofmokl[44], R.Holmes[1], S-O.Holmgren[38], D.Holthuisen[27], P.F.Honore[6], J.E.Hooper[26], M.Houlden[19], J.Hrubec[43], P.O.Hulth[38], K.Hultqvist[38], D.Husson[8], P.Ioannou[3], D.Isenhower[7], P-S.Iversen[4], J.N.Jackson[19], P.Jalocha[15], G.Jarlskog[21], P.Jarry[34], B.Jean-Marie[16], E.K.Johansson[38], D.Johnson[19], M.Jonker[7], L.Jonsson[21], P.Juillot[8], G.Kalkanis[3], G.Kalmus[32], F.Kapusta[20], S.Katsanevas[3], E.C.Katsoufis[28], R.Keranen[12], J.Kesteman[2], B.A.Khomenko[13], N.N.Khovanski[13], B.King[19], N.J.Kjaer[7], H.Klein[7], W.Klempt[7], A.Klovning[4], P.Kluit[27], A.Koch-Mehrin[45], J.H.Koehne[14], B.Koene[27], P.Kokkinias[9], M.Kopf[14], M.Koratzinos[39], K.Korcyl[15], A.V.Korytov[13], C.Kourkoumelis[3], T.Kreuzberger[43], J.Krolikowski[44], I.Kronkvist[21], J.Krstic[30], U.Kruener-Marquis[45], W.Krupinski[15], W.Kucewicz[25], K.Kurvinen[12], C.Lacasta[42], C.Lambropoulos[9], J.W.Lamsa[1], L.Lanceri[40], V.Lapin[37], J-P.Laugier[34], R.Lauhakangas[12], G.Leder[43], F.Ledroit[11], R.Leitner[7], Y.Lemoigne[34], J.Lemonne[2], G.Lenzen[45], V.Lepeltier[16], A.Letessier-Selvon[20], E.Lieb[45], D.Liko[43], E.Lillethun[4], J.Lindgren[12], A.Lipniacka[44], I.Lippi[31], R.Llosa[23], B.Loerstad[21], M.Lokajicek[13], J.G.Loken[30], A.Lopez-Fernandez[16], M.A.Lopez Aguera[36], M.Los[27], D.Loukas[9], A.Lounis[8], J.J.Lozano[42], P.Lutz[6], L.Lyons[30], G.Maehlum[7], N.Magnussen[45], J.Maillard[6], A.Maltezos[9], F.Mandl[43], J.Marco[36], M.Margoni[31], J-C.Marin[7], A.Markou[9], S.Marti[42], L.Mathis[1], F.Matorras[36], C.Matteuzzi[25], G.Matthiae[33], M.Matveev[37], M.Mazzucato[31], M.Mc Cubbin[19], R.Mc Kay[1], R.Mc Nulty[19], E.Menichetti[39], G.Meola[10], C.Meroni[25], W.T.Meyer[1], M.Michelotto[31], W.A.Mitaroff[43], G.V.Mitselmakher[13], U.Mjoernmark[21], T.Moa[38], R.Moeller[26], K.Moenig[7], M.R.Monge[10], P.Morettini[10], H.Mueller[14], W.J.Murray[32], B.Muryn[16], G.Myatt[30], F.Naraghi[20], U.Nau-Korzen[45], F.L.Navarria[5], P.Negri[25], B.S.Nielsen[26], B.Nijjhar[19], V.Nikolaenko[37], V.Obraztsov[37], K.Oesterberg[12], A.G.Olshevski[13], R.Orava[12], A.Ostankov[37], A.Ouraou[34], M.Paganoni[25], R.Pain[20], H.Palka[27], T.Papadopoulou[28], L.Pape[7], A.Passeri[35], M.Pegoraro[31], J.Pennanen[12], V.Perevoschikov[37], M.Pernicka[43], A.Perrotta[5], F.Pierre[34], M.Pimenta[18], O.Pingot[2], M.E.Pol[7], G.Polok[15], P.Poropat[40], P.Privitera[14], A.Pullia[25], D.Radojicic[30], S.Ragazzi[25], P.N.Ratoff[17], A.L.Read[29], N.G.Redaelli[25], M.Regler[43], D.Reid[19], P.B.Renton[30], L.K.Resvanis[3], F.Richard[16], M.Richardson[19], J.Ridky[13], G.Rinaudo[39], I.Roditi[7], A.Romero[39], I.Roncagliolo[10], P.Ronchese[31], V.Ronjin[37], C.Ronnqvist[12], E.I.Rosenberg[1], U.Rossi[5], E.Rosso[7], P.Roudeau[16], T.Rovelli[5], W.Ruckstuhl[27], V.Ruhlmann[34], A.Ruiz[36], K.Rybicki[15], H.Saarikko[12], Y.Sacquin[34], G.Sajot[11], J.Salt[42], E.Sanchez[42], J.Sanchez[23], M.Sannino[10], M.Schaeffer[8], S.Schael[14], H.Schneider[14], M.A.E.Schyns[7], F.Scuri[40], A.M.Segar[30], R.Sekulin[32], M.Sessa[40], G.Sette[10], R.Seufert[14], R.C.Shellard[7], P.Siegrist[34], S.Simonetti[10], F.Simonetto[31], A.N.Sissakian[13], T.B.Skaali[29], G.Skjevling[29], G.Smadja[34,22], G.R.Smith[32], R.Sosnowski[44],

T.S.Spassoff[11], E.Spiriti[35], S.Squarcia[10], H.Staeck[45], C.Stanescu[35], G.Stavropoulos[9], F.Stichelbaut[2], A.Stocchi[16], J.Strauss[43], R.Strub[8], M.Szczekowski[44], M.Szeptycka[44], P.Szymanski[44], T.Tabarelli[25], S.Tavernier[2], G.E.Theodosiou[9], A.Tilquin[24], J.Timmermans[27], V.G.Timofeev[13], L.G.Tkatchev[13], T.Todorov[13], D.Z.Toet[27], O.Toker[12], E.Torassa[39], L.Tortora[35], M.T.Trainor[30], D.Treille[7], U.Trevisan[10], W.Trischuk[7], G.Tristram[6], C.Troncon[25], A.Tsirou[7], E.N.Tsyganov[13], M.Turala[15], R.Turchetta[8], M-L.Turluer[34], T.Tuuva[12], I.A.Tyapkin[13], M.Tyndel[32], S.Tzamarias[7], B.Ueberschaer[45], S.Ueberschaer[45], O.Ullaland[7], V.Uvarov[37], G.Valenti[5], E.Vallazza[39], J.A.Valls Ferrer[42], C.Vander Velde[2], G.W.Van Apeldoorn[27], P.Van Dam[27], W.K.Van Doninck[2], J.Varela[18], P.Vaz[7], G.Vegni[25], L.Ventura[31], W.Venus[32], F.Verbeure[2], L.S.Vertogradov[13], D.Vilanova[34], L.Vitale[40], E.Vlasov[37], S.Vlassopoulos[28], A.S.Vodopyanov[13], M.Vollmer[45], S.Volponi[5], G.Voulgaris[3], M.Voutilainen[12], V.Vrba[35], H.Wahlen[45], C.Walck[38], F.Waldner[40], M.Wayne[1], P.Weilhammer[7], J.Werner[45], A.M.Wetherell[7], J.H.Wickens[2], J.Wikne[29], G.R.Wilkinson[30], W.S.C.Williams[30], M.Winter[8], D.Wormald[29], G.Wormser[16], K.Woschnagg[41], N.Yamdagni[38], P.Yepes[7], A.Zaitsev[37], A.Zalewska[15], P.Zalewski[16], D.Zavrtanik[7], E.Zevgolatakos[9], G.Zhang[45], N.I.Zimin[13], M.Zito[34], R.Zitoun[20], R.Zukanovich Funchal[6], G.Zumerle[31], J.Zuniga[42]

[1] Ames Laboratory and Department of Physics, Iowa State University, Ames IA 50011, USA
[2] Physics Department, Univ. Instelling Antwerpen, Universiteitsplein 1, B-2610 Wilrijk, Belgium
and IIHE, ULB-VUB, Pleinlaan 2, B-1050 Brussels, Belgium
and Service de Phys. des Part. Elém., Faculté des Sciences, Université de l'Etat Mons, Av. Maistriau 19, B-7000 Mons, Belgium
[3] Physics Laboratory, University of Athens, Solonos Str. 104, GR-10680 Athens, Greece
[4] Department of Physics, University of Bergen, Allégaten 55, N-5007 Bergen, Norway
[5] Dipartimento di Fisica, Università di Bologna and INFN, Via Irnerio 46, I-40126 Bologna, Italy
[6] Collège de France, Lab. de Physique Corpusculaire, 11 pl. M. Berthelot, F-75231 Paris Cedex 05, France
[7] CERN, CH-1211 Geneva 23, Switzerland
[8] Division des Hautes Energies, CRN - Groupe DELPHI and LEPSI, B.P.20 CRO, F-67037 Strasbourg Cedex, France
[9] Institute of Nuclear Physics, N.C.S.R. Demokritos, P.O. Box 60228, GR-15310 Athens, Greece
[10] Dipartimento di Fisica, Università di Genova and INFN, Via Dodecaneso 33, I-16146 Genova, Italy
[11] Institut des Sciences Nucléaires, Université de Grenoble 1, F-38026 Grenoble, France
[12] Research Institute for High Energy Physics, University of Helsinki, Siltavuorenpenger 20 C, SF-00170 Helsinki 17, Finland
[13] Joint Institute for Nuclear Research, Dubna, Head Post Office, P.O. Box 79, 101 000 Moscow, USSR.
[14] Institut für Experimentelle Kernphysik, Universität Karlsruhe, Postfach 6980, D-7500 Karlsruhe 1, FRG
[15] High Energy Physics Laboratory, Institute of Nuclear Physics, Ul. Kawiory 26 a, PL-30055 Krakow 30, Poland
[16] Université de Paris-Sud, Lab. de l'Accélérateur Linéaire, Bat 200, F-91405 Orsay, France
[17] School of Physics and Materials, University of Lancaster - Lancaster LA1 4YB, UK
[18] LIP, Av. Elias Garcia 14 - 1e, P-1000 Lisbon Codex, Portugal
[19] Department of Physics, University of Liverpool, P.O. Box 147, GB - Liverpool L69 3BX, UK
[20] LPNHE, Universités Paris VI et VII, Tour 33 (RdC), 4 place Jussieu, F-75230 Paris Cedex 05, France
[21] Department of Physics, University of Lund, Sölvegatan 14, S-22363 Lund, Sweden
[22] Université Claude Bernard de Lyon, 43 Bd du 11 Novembre 1918, F-69622 Villeurbanne Cedex, France
[23] Universidad Complutense, Avda. Complutense s/n, E-28040 Madrid, Spain
[24] Univ. d'Aix - Marseille II - Case 907 - 70, route Léon Lachamp, F-13288 Marseille Cedex 09, France
[25] Dipartimento di Fisica, Università di Milano and INFN, Via Celoria 16, I-20133 Milan, Italy
[26] Niels Bohr Institute, Blegdamsvej 17, DK-2100 Copenhagen 0, Denmark
[27] NIKHEF-H, Postbus 41882, NL-1009 DB Amsterdam, The Netherlands
[28] National Technical University, Physics Department, Zografou Campus, GR-15773 Athens, Greece
[29] Physics Department, University of Oslo, Blindern, N-1000 Oslo 3, Norway
[30] Nuclear Physics Laboratory, University of Oxford, Keble Road, GB - Oxford OX1 3RH, UK
[31] Dipartimento di Fisica, Università di Padova and INFN, Via Marzolo 8, I-35131 Padua, Italy
[32] Rutherford Appleton Laboratory, Chilton, GB - Didcot OX11 OQX, UK
[33] Dipartimento di Fisica, Università di Roma II and INFN, Tor Vergata, I-00173 Rome, Italy
[34] CEN-Saclay, DPhPE, F-91191 Gif-sur-Yvette Cedex, France
[35] Istituto Superiore di Sanità, Ist. Naz. di Fisica Nucl. (INFN), Viale Regina Elena 299, I-00161 Rome, Italy
[36] Facultad de Ciencias, Universidad de Santander, av. de los Castros, E - 39005 Santander, Spain
[37] Inst. for High Energy Physics, Serpukow P.O. Box 35, Protvino, (Moscow Region), USSR.
[38] Institute of Physics, University of Stockholm, Vanadisvägen 9, S-113 46 Stockholm, Sweden
[39] Dipartimento di Fisica Sperimentale, Università di Torino and INFN, Via P. Giuria 1, I-10125 Turin, Italy
[40] Dipartimento di Fisica, Università di Trieste and INFN, Via A. Valerio 2, I-34127 Trieste, Italy
and Istituto di Fisica, Università di Udine, I-33100 Udine, Italy
[41] Department of Radiation Sciences, University of Uppsala, P.O. Box 535, S-751 21 Uppsala, Sweden
[42] Inst. de Fisica Corpuscular IFIC, Centro Mixto Univ. de Valencia-CSIC, and Departamento de Fisica Atomica Molecular y Nuclear, Univ. de Valencia, Avda. Dr. Moliner 50, E-46100 Burjassot (Valencia), Spain
[43] Institut für Hochenergiephysik, Öesterreich Akad. d. Wissensch., Nikolsdorfergasse 18, A-1050 Vienna, Austria
[44] Inst. Nuclear Studies and, University of Warsaw, Ul. Hoza 69, PL-00681 Warsaw, Poland
[45] Fachbereich Physik, University of Wuppertal, Postfach 100 127, D-5600 Wuppertal 1, FRG

1 Introduction

The study of the production of strange particles with different quark flavors and spins can be used to examine the underlying dynamics of jet fragmentation, as well as the coupling of the Z^0 to $s\bar{s}$ pairs.

The production of the strange particles K^0_S, $K^{*\pm}$, $\Lambda(\bar{\Lambda})$, and $\Xi^-(\bar{\Xi}^+)$ has been analysed using data collected by the DELPHI detector [1] at the e^+e^- storage ring LEP at CERN. The data were taken around the Z^0 peak in 1990.

The cross section measurements are compared with the predictions of the JETSET 7.2 Monte Carlo model (using parton shower generation and string fragmentation) with parameters tuned to data at PEP/PETRA energies [2].

2 Experimental procedure and event selection

The sample of events used in the analysis was collected by the DELPHI detector at the LEP e^+e^- collider during 1990. A description of the DELPHI detector can be found elsewhere [1]. Features of the apparatus relevant for the analysis of multihadronic final states (with emphasis on the detection of charged particles) are outlined in reference [3]. The present analysis relies mainly on the information provided by the central tracking detectors:

- The Inner Detector (ID): a cylindrical drift chamber (inner radius 12 cm and outer radius 22 cm) covering polar angles between 29° and 151°.
- The Time Projection Chamber (TPC): a cylinder with 28 cm inner and 122 cm outer radius and a length of 2.7 m. For a polar angle θ between 22° and 158° at least 4 space points are available for track reconstruction, while for angles between 39° and 141° up to 16 space points can be used.
- The Outer Detector (OD): 5 layers of drift cells at a radius between 192 and 208 cm, covering polar angles between 50° and 130°.
- The Microvertex Detector (VD): two cylindrical layers of silicon microstrip detectors at radii 9 and 11 cm covering polar angles between 45° and 135°. This detector was not fully implemented in this analysis and was used only to find the position of the primary interaction region.

In addition, a determination of the $K^\pm$ cross section for momenta between 1 and 2 GeV/c has been obtained from the measurement of the $\pi^\pm/K^\pm$ ratio using the Barrel RICH (Ring Imaging Cherenkov) detector. The Barrel RICH [1] covers the polar angle between 40° and 140°. It identifies the charged particles by measuring the angle of emission of Cherenkov light, and thus the velocity. The mass of the charged particle is then extracted by using the velocity information combined with the momentum measurement. In order to cover a large momentum range (1 to 20 GeV/c), the DELPHI Barrel RICH uses two different Cherenkov radiators; one liquid (C_6F_{14}) and one gaseous (C_5F_{12}). Only the liquid radiator was operational during 1990, and for only one tenth of the data taking.

Measurements from the TPC, ID and OD, taken together, provide a complete coverage for θ between 25° and 155°, with reconstruction efficiency near to 1. The average momentum resolution $\Delta p/p$ varies from 0.005 to $0.01p$ (p in GeV/c), depending on θ.

Charged particles were used in the analysis if they had:

(a) momentum p larger than 0.1 GeV/c;

(b) measured track length in the TPC above 30 cm;
(c) θ between 25° and 155°.
Hadronic events were then selected by requiring that:
(α) the total energy of the charged particles in each hemisphere (θ above and below 90°) exceeded 3 GeV;
(β) the total energy of the charged particles exceeded 15 GeV;
(γ) there were at least 5 charged particles with momenta above 0.2 GeV/c.
In the calculation of the energies, all charged particles have been assumed to have the pion mass.

A total of 86,948 events satisfied these cuts. Events due to beam-gas scattering and to $\gamma\gamma$ interactions have been estimated to be less than 0.1% of the sample; background from $\tau^+\tau^-$ events was calculated to be less than 0.2%.

The mean position of the primary Z^0 decay vertex has been measured for each fill using the VD data [4]. The typical resolution on the impact parameters of tracks is about 0.015 cm in the plane perpendicular to the beam axis when using their VD data and about 0.05 cm when the VD data are not used.

The influence of the detector on the analysis was studied with the simulation programme DELSIM [5]. Events were generated using the JETSET 7.2 Parton Shower Monte Carlo programme [2] (JETSET PS in the following) with default parameters. The particles were followed through the detailed geometry of DELPHI giving simulated digitizations in each detector. These data were processed with the same reconstruction and analysis programmes as the real data.

3 Analysis and Results

3.1 K^0_S production

$K^0_S \to \pi^+\pi^-$ decays are detected at the secondary vertex separated from the primary Z^0 decay. Candidate secondary vertices, V_K, were found by considering the tracks of all pairs of oppositely charged particles. The vertex defined by each such pair was determined such that the χ^2 obtained from the distance of the vertex to the extrapolated tracks was minimised. Most candidate vertices are not formed by strange particle decay and were rejected by ensuring the following:

- In the xy plane (perpendicular to the beam axis), the sine of the angle between the vector sum of the charged particle momenta and the line joining the primary to the secondary vertex was less than 0.04.
- The impact parameters in the xy plane of both tracks projected to the primary vertex had to be greater than 0.15 cm and at least one greater than 0.5 cm.
- The separation in z (beam axis) of the two tracks was less than 0.5 cm. In case of two intersections in the xy plane, the solution with smaller distance in z was chosen.
- The separation of the primary and secondary vertex in the xy plane was greater than 1.5 cm.

The remaining secondary vertices include two types of background to K^0_S: that coming from other decays, secondary interactions or photon conversions, and that coming from random associations of badly measured primary charged particles and particles from separate secondary vertices. Photon conversions and Λ decays were effectively removed by requiring that the transverse momentum of the decay products relative to their vector sum was greater than 0.1 GeV/c. This also removes a small fraction of the K^0_S signal.

The $\pi^+\pi^-$ invariant mass spectrum from the accepted V_K candidates is shown in Figure 1; a clear K^0_S signal is seen over a small background, below 10% at the peak. The background due to random associations of badly measured primary particles is reduced to about 1% in the part of the sample where the measurement precision is improved using hits in the VD. However this analysis does not use the VD information for reconstructing secondary vertices because many K^0_S decay beyond the VD and it was efficient for only a fraction of the two decay particles in the 1990 data.

The spectrum has been fitted using the MINUIT [6] package to a linear background function and a sum of two Gaussians for the signal in the range from 0.35 GeV/c^2 to 0.65 GeV/c^2. The fit gives a total of $9411 \pm 94\,(stat) \pm 34\,(sys)$ K^0_S, and $m_{K^0_S} = 496.6 \pm 0.2\,(stat) \pm 2.1\,(sys)$ MeV/c^2. The systematic error on the mass is due to the uncertainty on the energy loss of the pions while crossing the material in the detector, and to the choice of the parametrization in the fit*. The measured K^0 mass is consistent with the world average of 497.67 ± 0.03 MeV/c^2[7]. The resolution of about 8 MeV/c^2 is a function of momentum and cannot be adequately described by a single Gaussian.

In order to calculate differential cross sections, the background was evaluated as a function of the kinematical variables and was subtracted throughout the following analysis. The efficiency for $K^0_S \to \pi^+\pi^-$ reconstruction was evaluated from the simulated data. As a check of these procedures, the K^0_S lifetime, $\tau_{K^0_S}$, was measured. The distribution of the proper decay times t of the reconstructed K^0_S was corrected by the efficiencies for reconstructing simulated K^0_S, and then fitted by least squares to an exponential decay function $Aexp(-t/\tau_{K^0_S})$. This gave $\tau_{K^0_S} = 89.6 \pm 1.9$ ps (the error is statistical only), consistent with the world average of 89.2 ± 0.2 ps[7].

The reconstruction efficiency is tabulated in Table 1 as a function of the particle fractional momentum $x_p = 2p/\sqrt{s}$ in the region up to $x_p = 0.4$. The differential cross section $(1/\sigma_h)(d\sigma/dx_p)$ (where σ_h is the cross section for $e^+e^- \to Z^0 \to hadrons$) for inclusive K^0 and $\bar{K}^0$ production at the Z^0 peak was measured by repeating the background subtraction procedure in each momentum bin and correcting for the reconstruction efficiency and unseen K^0 decay modes. The results are given in Table 1, and plotted in Figure 2. The prediction from JETSET PS reproduces the measurement reasonably well.

The mean $K^0(\bar{K}^0)$ multiplicity, $< N_{K^0} > + < N_{\bar{K}^0} >$, was obtained by integrating the distribution as a function of x_p for x_p between 0.005 and 0.30, and assuming the unmeasured regions are represented by the normalised JETSET PS prediction. This gave

$$< N_{K^0} > + < N_{\bar{K}^0} > = 2.12 \pm 0.05\,(stat) \pm 0.04\,(sys)\,, \qquad (1)$$

in agreement with the OPAL result[8].

Finally, from the K^0 differential cross section, the ratio γ_s/γ_u of the probability of exciting a $s\bar{s}$ pair from the vacuum to the probability of exciting a $u\bar{u}$ (or $d\bar{d}$) has been determined by tuning this parameter in JETSET PS to best fit the data. A value

$$\frac{\gamma_s}{\gamma_u} = 0.30 \pm 0.02\,(stat) \qquad (2)$$

has been obtained. In this analysis it was assumed that the reconstruction efficiency was a function of x_p only, and was not dependent on the origin of the K^0_S. The measurement also assumes that the production of K^0 from B and D decays is correctly modelled in JETSET PS. The result of the fit was found to be stable when varying the fraction of $s\bar{s}$ events in JETSET PS to the total number of hadronic events from 0.1 to 0.5. This result is consistent with measurements in e^+e^- interactions at lower energies [9].

*The systematic error includes contributions from varying the fit by choosing: a third-order polynomial or an exponential to represent the background, and changing the bin size and the mass range.

$x_p = \frac{2p}{\sqrt{s}}$	Efficiency (%)	$(\frac{1}{\sigma_h}\frac{d\sigma}{dx_p})$
0.005 - 0.025	6.7 ±0.3	19.5±1.4
0.025 - 0.045	18.0±0.6	18.1±0.8
0.045 - 0.065	22.9±0.8	13.1±0.6
0.065 - 0.085	22.7±0.9	10.1±0.5
0.085 - 0.105	20.8±1.0	7.5±0.5
0.105 - 0.125	18.2±1.1	6.4±0.5
0.125 - 0.145	16.7±1.1	4.4±0.4
0.145 - 0.165	13.5±1.2	4.5±0.5
0.165 - 0.185	12.8±1.3	3.4±0.4
0.185 - 0.205	11.0±1.4	2.7±0.4
0.205 - 0.225	8.5±1.4	2.5±0.5
0.225 - 0.245	9.2±1.6	2.2±0.5
0.245 - 0.265	7.8±1.7	1.6±0.5
0.265 - 0.285	3.8±1.5	1.5±1.1
0.285 - 0.305	4.5±1.8	0.8±0.6
0.305 - 0.405	3.2±1.0	0.8±0.5

Table 1: *Efficiency for $K^0_S \to \pi^+\pi^-$ and differential cross sections for K^0 production, as a function of the fractional momentum x_p.*

3.2 $K^{\pm}$ production

The measured Cherenkov angle distribution from the Barrel RICH is plotted in Figure 3a against the particle momentum. The peaks corresponding to pions, kaons and protons are clearly visible in the mass plot in Figure 3b for momenta between 1 and 2 GeV/c. The corresponding measurement of the $K^{\pm}$ cross section is shown in Figure 2. This point includes a relative systematic error of 20% added in quadrature, to account for the uncertainty on possible differences in K and π identification efficiencies. The average $(K^+ + K^-)$ multiplicity in the range of momentum used for the measurement agrees with the average $(K^0 + \bar{K}^0)$ multiplicity.

3.3 $K^{*\pm}$ production

The $K^{*\pm}$ is detected by its decay to $K^0_S\pi^{\pm}$ with the subsequent decay $K^0_S \to \pi^+\pi^-$. K^0_S are selected to lie within three standard deviation of the peak of the $\pi^+\pi^-$ invariant mass distribution. These K^0_S candidates are fitted by constraining the pions to make the nominal K^0 mass and then combined with all remaining charged particles in the event.

Figure 4 shows the $K^0_S\pi^{\pm}$ mass distribution; a clear K^* signal is seen. The distribution has been fitted between 0.65 and 1.5 GeV/c^2 with the expression

$$\begin{aligned} \frac{dN}{dm} &= a_1 \,.\, BG \,+\, a_2 \,.\, BW_{K^*} \qquad \text{where} \\ BG &= (m - m_{\pi^{\pm}} - m_{K^0})^{a_3} \,.\, exp(a_4 m + a_5 m^2 + a_6 m^3) \\ BW_{K^*} &= \frac{m}{q} \cdot \frac{\Gamma'_{K^*}}{(m^2 - m^2_{K^*})^2 + (m_{K^*}\Gamma'_{K^*})^2} \qquad \text{and} \end{aligned}$$

$$\Gamma'_{K^*} = \Gamma_{K^*} \cdot \left(\frac{q}{q_{K^*}}\right)^3 \cdot \frac{m_{K^*}}{m}$$

BG represents the chosen background parametrisation and BW_{K^*} the relativistic Breit-Wigner function with mass dependent width corresponding to a p-wave. m_{K^*} is the central mass value of the K^* and Γ_{K^*} the width. m is the mass of the $K\pi$ system, q the pion momentum in the $K\pi$ rest frame and the a_i are free parameters. The results of the fit are $m_{K^*} = 892 \pm 4\,\mathrm{MeV/c^2}$ and $\Gamma_{K^*} = 43 \pm 12$ MeV/c^2. The mass is consistent with the world average of 891.8 ± 0.2 MeV/c^2[7], while the width includes a contribution of some 10 MeV/c^2 due to the mass resolution.

The average multiplicity for $K^{*\pm}$ production has been measured to be

$$< N_{K^{*+}} > + < N_{K^{*-}} > = 1.33 \pm 0.11\,(stat) \pm 0.24\,(sys)\,, \qquad (3)$$

by following the same procedure discussed in section 3.1 for K^0_S to evaluate efficiency and acceptance, to extrapolate the cross section in the unobserved momentum region, and to correct for the unobserved decay modes. The systematic error comes from two approximately equal contributions, the choice of the background shape and the interval used for the fit.

Finally, the relative probability R of producing a prompt strange meson with spin 1 has been measured by a fit using JETSET PS. This probability is a free parameter in most of the fragmentation models. The result is

$$R = 0.70 \pm 0.18\,. \qquad (4)$$

The measurement assumes also that the production of $K^{*\pm}$ from B and D decays is correctly modelled in JETSET PS. According to simple spin-statistics, R should be equal to 3/4, but a value $\simeq 0.5$ seems experimentally favoured at lower energies [10]. The present level of accuracy is not adequate to distinguish between the various hypotheses.

3.4 Λ production

The $\Lambda(\bar{\Lambda})$ baryon can be detected by its decay in flight into $p\pi^-$. The Λ decay vertex candidates were chosen to satisfy the following requirements:

- In the xy plane (perpendicular to the beam axis), the angle between the vector sum of the charged particle momenta and the line joining the primary to the secondary vertex was less than 1^o.
- The impact parameters in the xy plane of both tracks projected to the primary vertex had to be greater than 0.05 cm and at least one greater than 0.5 cm.
- The radial separation of the primary and secondary vertex in the xy plane was greater than 3 cm.

Ambiguities occur with K^0 decays into $\pi^+\pi^-$ and with conversions of photons to e^+e^- pairs. The K^0_S background was reduced by rejecting pπ candidates whose mass, when taken as $\pi\pi$, was less than 3 standard deviations from the K^0_S mass. Photon conversion to e^+e^- pairs were excluded by requiring their mass to be greater than 0.1 GeV/c^2 for the e^+e^- hypothesis and by requiring both particles to have transverse momentum larger than 0.02 GeV/c with respect to their vector sum.

The $p\pi^-(\bar{p}\pi^+)$ invariant mass spectrum from the accepted V_Λ candidates is shown in Figure 5; a clear $\Lambda(\bar{\Lambda})$ signal is seen, with resolution of about 2.5 MeV/c^2. The spectrum

$x_p = \frac{2p}{\sqrt{s}}$	Efficiency (%)	$(\frac{1}{\sigma_h}\frac{d\sigma}{dx_p})$
0.01 - 0.04	3.8±0.4	3.30±0.44
0.04 - 0.06	8.5±0.6	2.75±0.27
0.06 - 0.09	10.6±0.8	1.60±0.15
0.09 - 0.12	10.9±0.9	1.09±0.12
0.12 - 0.15	8.6±1.0	0.84±0.11
0.15 - 0.20	7.7±1.3	0.46±0.13

Table 2: *Efficiency and differential cross section for* $\Lambda(\bar{\Lambda})$ *production, as a function of the fractional momentum* x_p.

has been fitted by a sum of two Gaussian functions for the signal and a linear background in the range from 1.1 to 1.18 GeV/c^2. The fit gives $m_\Lambda = 1115.0 \pm 0.5\,(stat) \pm 0.9\,(sys)$ MeV/c^2, (consistent with the world average of 1115.63 $\pm$ 0.05 MeV/c^2[7]), and a total of 1915 $\pm$ 69 $(stat)$ $\pm$ 227 (sys) Λ. The systematic uncertainty includes the same contributions as that for the K^0_s mass measurement. The Λ lifetime, τ_Λ, has been determined from the selected sample. The correction factors for each bin of proper time are calculated from the simulation. A least-square fit of the corrected experimental distribution to an exponential decay function gives $\tau_\Lambda = 268 \pm 10$ ps (the error is statistical only), consistent with the world average of 263 $\pm$ 2 ps[7].

The momentum dependent efficiency for $\Lambda(\bar{\Lambda})$ reconstruction, including detector acceptance effects, has been calculated by simulation. The background was subtracted for each x_p region and the overall efficiency was calculated as in the K^0 analysis. The differential cross section $(\frac{1}{\sigma_h})(\frac{d\sigma}{dx_p})$ for inclusive Λ and $\bar{\Lambda}$ production at the Z^0 is shown in Table 2. The errors on the efficiency and on the differential cross section include both the statistical and the systematic contributions; the systematic error comes mainly from the parametrization of the background in the fit of the signal in Figure 5. In Figure 2 the measured cross section is compared with the prediction from JETSET PS.

Using JETSET PS to extrapolate the cross section to the unobserved momentum regions and correcting for unseen Λ decay modes, the total average $\Lambda(\bar{\Lambda})$ multiplicity has been determined to be

$$< N_\Lambda > + < N_{\bar{\Lambda}} > = 0.36 \pm 0.03\,(stat) \pm 0.06\,(sys)\,. \qquad (5)$$

The systematic error reflects the uncertainties due to the calculated efficiency and acceptance, the choice of the background parametrization, and the JETSET PS extrapolation. Λ production by Σ^0 decay is included in this total multiplicity.

The cross section for inclusive Λ or $\bar{\Lambda}$ production is sensitive to the probability of producing a strange di-quark in the fragmentation process. In the Lund string fragmentation model, this probability is related to the value assigned to the strange di-quark suppression parameter δ , defined as: $\delta = (P(us)/P(ud))/(P(s)/P(d))$.

The parameter δ was estimated by fitting the theoretical cross section, predicted by JETSET PS, to the experimental data on the differential $\Lambda(\bar{\Lambda})$ cross section. By using the same procedure described for the tuning of γ_s/γ_u, a result

$$\delta = 0.34 \pm 0.07\,(stat) \qquad (6)$$

was obtained. This result agrees within errors with the default value in JETSET PS ($\delta = 0.4$), tuned on experiments at PEP/PETRA energies. In the fit, the value of γ_s/γ_u was kept fixed to 0.3.

3.5 Ξ^- production

The Ξ^- (or $\bar{\Xi}^+$) baryon can be detected by its cascade decay chain $\Xi \rightarrow \Lambda\pi$, $\Lambda \rightarrow p\pi$. In order to enrich the Λ sample with Ξ decay products, the $\Lambda \rightarrow p\pi$ decay is reconstructed requiring:

- The distance of closest approach between the proton and pion trajectories in the xy plane must be less than 7mm, and at this point, their z separation must also be less than 7mm.
- The separation between the Z^0 decay and the candidate V_Λ vertex in the xy plane must exceed 40 mm.
- The transverse momentum of the Λ decay product candidates must be between 40 and 105 MeV/c with respect to their vector sum.

Only the Λ candidates with invariant mass between 1105 and 1125 MeV/c^2 were kept for the further analysis, and all the combinations from this region were assigned the nominal Λ mass. Each Λ candidate was paired with every negatively charged particle to make a Ξ^- candidate. The intersection in the xy plane was found between the straight line representing the Λ flight path and the circle representing the π trajectory. This Ξ^- decay vertex candidate must satisfy the following requirements:

- The distance in the z direction between the tracks at the intersection of their projections in the xy plane must be less than 8 mm.
- The separation between the Z^0 decay and the candidate Ξ^- decay vertex in the xy plane must exceed 30 mm.
- The impact parameter of the Ξ^- trajectory (determined by summing its decay products) to the production vertex must be less than 6mm in the xy plane.
- the transverse momentum of the Λ and π must be larger than 0.05 GeV/c with respect to their sum.

Figure 6a shows the masses of the resulting right-sign $\Lambda\pi$ combinations $(\Lambda\pi^-, \bar{\Lambda}\pi^+)$ and figure 6b the wrong-sign $(\Lambda\pi^+, \bar{\Lambda}\pi^-)$ combinations. The narrow peak in Figure 6a corresponds to Ξ production. The spectrum has been fitted to a Gaussian function for the signal with a linear background. The fit gives $m_\Xi = 1319.0 \pm 0.7\,(stat) \pm 1.2\,(sys)$ MeV/c^2, (consistent with the world average of 1321.3 $\pm$ 0.1 MeV/c^2[7]) and a Gaussian width of 4.2 $\pm$ 0.6 MeV/c^2 representing the mass resolution.

The overall efficiency for $\Xi^-(\bar{\Xi}^+)$ reconstruction includes corrections for unseen decays modes of the Λ, and the detector effects estimated from the simulation. The average Ξ multiplicity has been determined to be:

$$< N_{\Xi^-} > + < N_{\bar{\Xi}^+} >= 0.020 \pm 0.004\,(stat) \pm 0.003\,(sys)\,, \qquad (7)$$

consistent with JETSET PS of approximately 0.025. From a total of $132 \pm 20\,(stat) \pm 20\,(sys)$ $\Xi^-(\bar{\Xi}^+)$, the measured differential cross section $(1/\sigma_h)(d\sigma/dx_\Xi)$ for inclusive Ξ production at the Z^0 peak is tabulated in Table 3 and plotted in Figure 2.

3.6 Comparison of the cross sections for strange particles

A useful framework for comparing the differential cross sections for the production of different particles is given by QCD calculations in the Modified Leading Log Approximation [11,12] (MLLA). Such analyses have already been performed at LEP on π^0 [13] and K^0 [8] spectra.

$x_p = \frac{2p}{\sqrt{s}}$	Efficiency (%)	$(\frac{1}{\sigma_h}\frac{d\sigma}{dx_p})$
0.00 - 0.10	6.6±1.0	0.110 ±0.025
0.10 - 0.20	10.5±2.1	0.040 ±0.013
0.20 - 0.30	5.5±2.4	0.035 ±0.019
0.30 - 0.50	3.7±2.1	0.009 ±0.007

Table 3: *Efficiency and differential cross sections for $\Xi^-(\bar{\Xi}^+)$ production, as a function of the fractional momentum x_p.*

In Figure 7, the production cross sections for Λ, K^0 and all charged particles are plotted as a function of the variable $\xi_p = \ln 1/x_p$.

The results of the MLLA calculation depend on an effective QCD scale Λ_{eff} and on a cutoff of the parton cascade Q_0 which is expected to grow with growing masses of the particles produced. The position ξ^* of the maxima of the distribution is expected to decrease as the mass of the produced particle increases. When fitting $\frac{d\sigma}{d\xi_p}$, for ξ_p within 1 of the maximum, to a distorted Gaussian [14], the following results are obtained:

$$\begin{aligned} \xi^*_{all\,charged} &= 3.67 \pm 0.10 \\ \xi^*_{K^0} &= 2.62 \pm 0.11 \\ \xi^*_{\Lambda} &= 2.82 \pm 0.25 \end{aligned}$$

where the errors allow for the choice of different ranges for the fit[†].

The position of the maximum is observed to be lower for kaons and lambdas than for all charged particles; no difference is seen within the accuracy of the measurement between the maxima of kaons and lambdas.

The positions of the peaks, assuming $\Lambda_{eff} = 0.15$ GeV, correspond through the calculations in reference [12] to

$$\begin{aligned} Q_0(all\,charged) &\simeq 0.15 \pm 0.02\,\mathrm{GeV} \\ Q_0(K^0) &\simeq 0.43 \pm 0.04\,\mathrm{GeV} \\ Q_0(\Lambda) &\simeq 0.35 \pm 0.10\,\mathrm{GeV}\,. \end{aligned}$$

4 Summary and Conclusions

The inclusive production of strange particles has been analysed from a sample of $\simeq$ 90,000 hadronic Z^0 decays collected by the DELPHI detector at LEP.

The following average multiplicities for strange particles have been measured:

$$\begin{aligned} < N_{K^0} > + < N_{\bar{K}^0} > &= 2.12 \pm 0.07 \\ < N_{K^{*+}} > + < N_{K^{*-}} > &= 1.33 \pm 0.26 \\ < N_{\Lambda} > + < N_{\bar{\Lambda}} > &= 0.36 \pm 0.07 \\ < N_{\Xi^-} > + < N_{\bar{\Xi}^+} > &= 0.020 \pm 0.005 \end{aligned}$$

where statistical and systematic errors have been summed in quadrature.

[†]The bin sizes chosen for the differential Λ cross section are different from those tabulated in Table 2, in order to increase the sensitivity in the low-x_p region.

The predictions of the JETSET 7.2 version of the Lund Monte Carlo program, as tuned from the data at PEP/PETRA energies, are consistent with these results on total and differential cross sections.

The ratio γ_s/γ_u of the probability of exciting a $s\bar{s}$ pair from the vacuum to the probability of exciting a $u\bar{u}$ (or $d\bar{d}$), and the strange di-quark suppression factor δ, have been found to be consistent with measurements in e^+e^- interactions at lower energies.

Acknowledgements

We want to thank V. Khoze, T. Sjöstrand and especially Yuri Dokshitzer for clarifying discussions. We are greatly indebted to our technical collaborators and to the funding agencies for their support in building and operating the DELPHI detector, and to the members of the CERN-SL Division for the excellent performance of the LEP collider.

References

[1] P. Aarnio et al. (DELPHI Collaboration), Nucl. Instr. and Meth. **A303** (1991) 233.

[2] T. Sjöstrand et al., "The Lund Monte Carlo Programs", CERN, 1 November 1989.
T. Sjöstrand, Comp. Phys. Comm. **27** (1982) 243, ibid. **28** (1983) 229.
T. Sjöstrand and M. Bengtsson, Comp. Phys. Comm. **43** (1987) 367.

[3] P. Aarnio et al. (DELPHI Collaboration), Phys. Lett. **B240** (1990) 271.

[4] P. Abreu et al. (DELPHI Collaboration), CERN-PPE/91-131, to be published in Zeit. Phys. C.

[5] DELSIM User Manual, DELPHI 87-96 PROG-99, CERN, July 1989.
DELSIM Reference Manual, DELPHI 87-98 PROG-100, CERN, July 1989.

[6] F.James and M.Roos, CERN Program Library D506.
MINUIT - Function Minimization and Error Analysis.

[7] Review of Particle Properties, Particle Data Group, Phys. Lett. **B239** (1990).

[8] G.Alexander et al. (OPAL Collaboration), Phys. Lett. **B264** (1991) 219.

[9] P.K. Malhotra and R. Orava, Z. Phys. **C17** (1983) 85.
A. Wroblewski, Acta Physica Polonica **B16** (1985) 379.

[10] P.V. Chliapnikov and V.A. Uvarov, Phys. Lett. **B240** (1990) 519.

[11] Ya.I. Azimov et al., Z. Phys. **C27** (1985) 213 and **C31** (1986) 213.
Yu.L.Dokshitzer et al., in "Basics of Perturbative QCD", ed.A.Mueller, Editions Frontieres, Paris, 1991.

[12] Yu.L.Dokshitzer et al. LU TP 91-12 (1991), to appear in Int. J. Mod. Phys. A.

[13] B.Adeva et al. (L3 Collaboration), Phys. Lett. **B259** (1991) 119.

[14] C.P. Fong and B.R. Webber, Phys. Lett. **B229** (1989) 289.

Figure captions

1. $\pi^+\pi^-$ invariant mass spectrum for secondary decay candidates.
2. Differential cross section $(1/\sigma_h)(d\sigma/dx_p)$ for production of: all charged particles - circles, $(K^0 + \bar{K}^0)$ - triangles, $(\Lambda + \bar{\Lambda})$ - squares, $(\Xi^- + \bar{\Xi}^+)$ - diamonds, versus the fractional momentum x_p. Curves are for JETSET PS with default parameters.
3. (a) Measured Cherenkov angle in Barrel RICH versus the momentum of the incident particle (GeV/c).
   (b) Distribution of the calculated mass for charged particles with momenta between 1 and 2 GeV/c.
4. $K^0_S\pi^\pm$ invariant mass spectrum. The dotted curve shows the fitted K^* signal and the dashed curve the fitted background.
5. $p\pi$ invariant mass spectrum for secondary decay candidates.
6. $\Lambda\pi$ invariant mass for secondary decay candidates with (a) right and (b) wrong sign combinations. The curve on figure 6a is the result of the fit.
7. Comparison of the cross sections for K^0, Λ and all charged particles as a function of ξ_p. The curves correspond to fits near the maxima using a distorted Gaussian function (see text).

Figure 1.

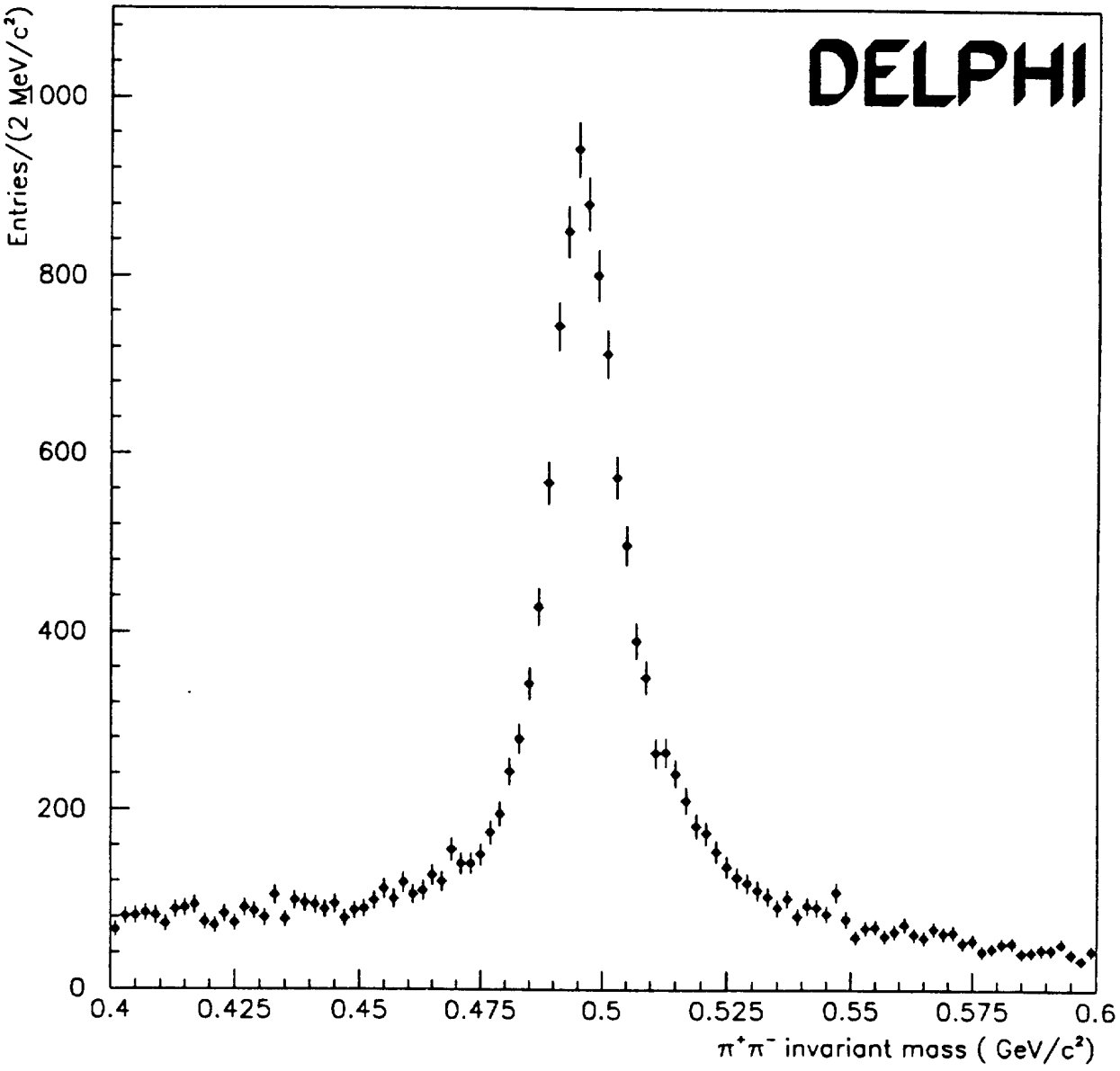
DELPHI
Entries/(2 MeV/c²)
0
200
400
600
800
1000
0.4
0.425
0.45
0.475
0.5
0.525
0.55
0.575
0.6
π⁺π⁻ invariant mass (GeV/c²)

Figure 2

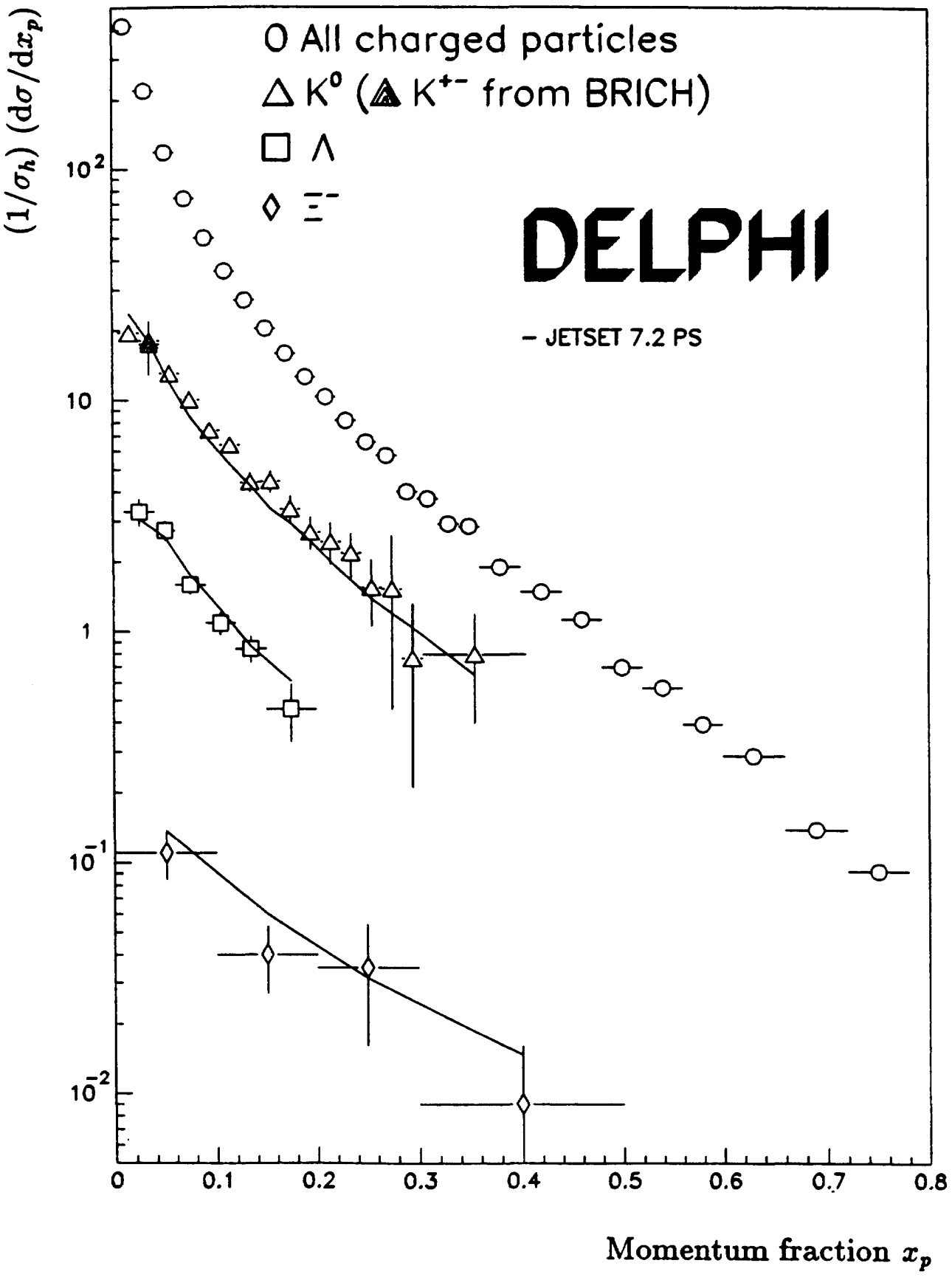
O All charged particles
Δ K⁰ (▲ K⁺⁻ from BRICH)
□ Λ
◊ Ξ⁻
DELPHI
– JETSET 7.2 PS
$(1/\sigma_h)\ (d\sigma/dx_p)$
10^2
10
1
10^{-1}
10^{-2}
0
0.1
0.2
0.3
0.4
0.5
0.6
0.7
0.8
Momentum fraction x_p

Figure 3

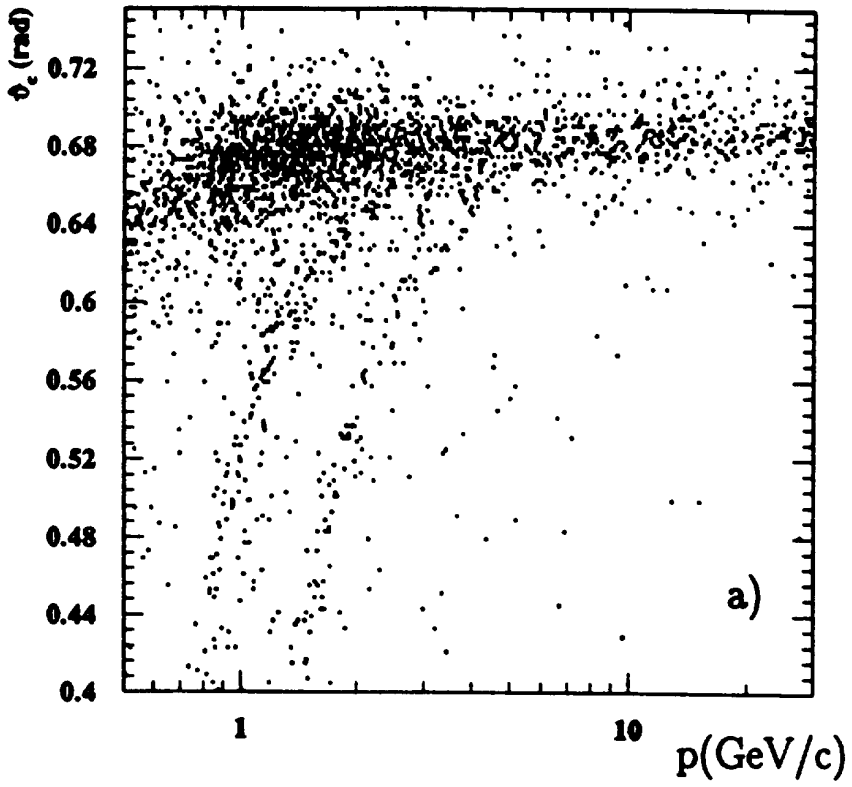
Φ_c (rad)
0.72
0.68
0.64
0.6
0.56
0.52
0.48
0.44
0.4
1
10
p(GeV/c)
a)

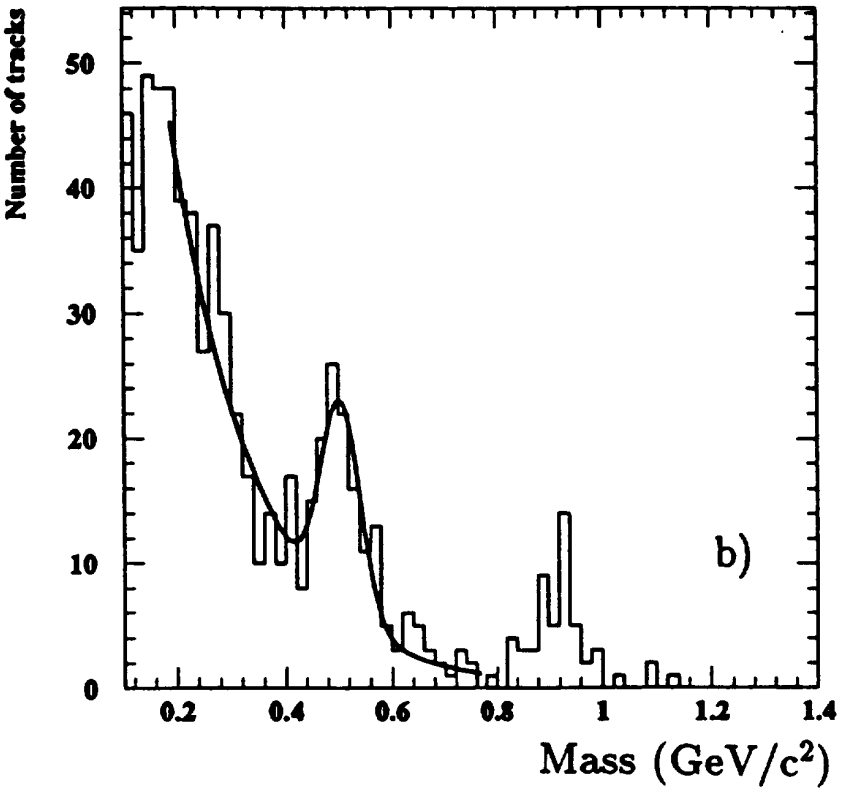
Number of tracks
50
40
30
20
10
0
0.2
0.4
0.6
0.8
1
1.2
1.4
Mass (GeV/c^2)
b)

Figure 4

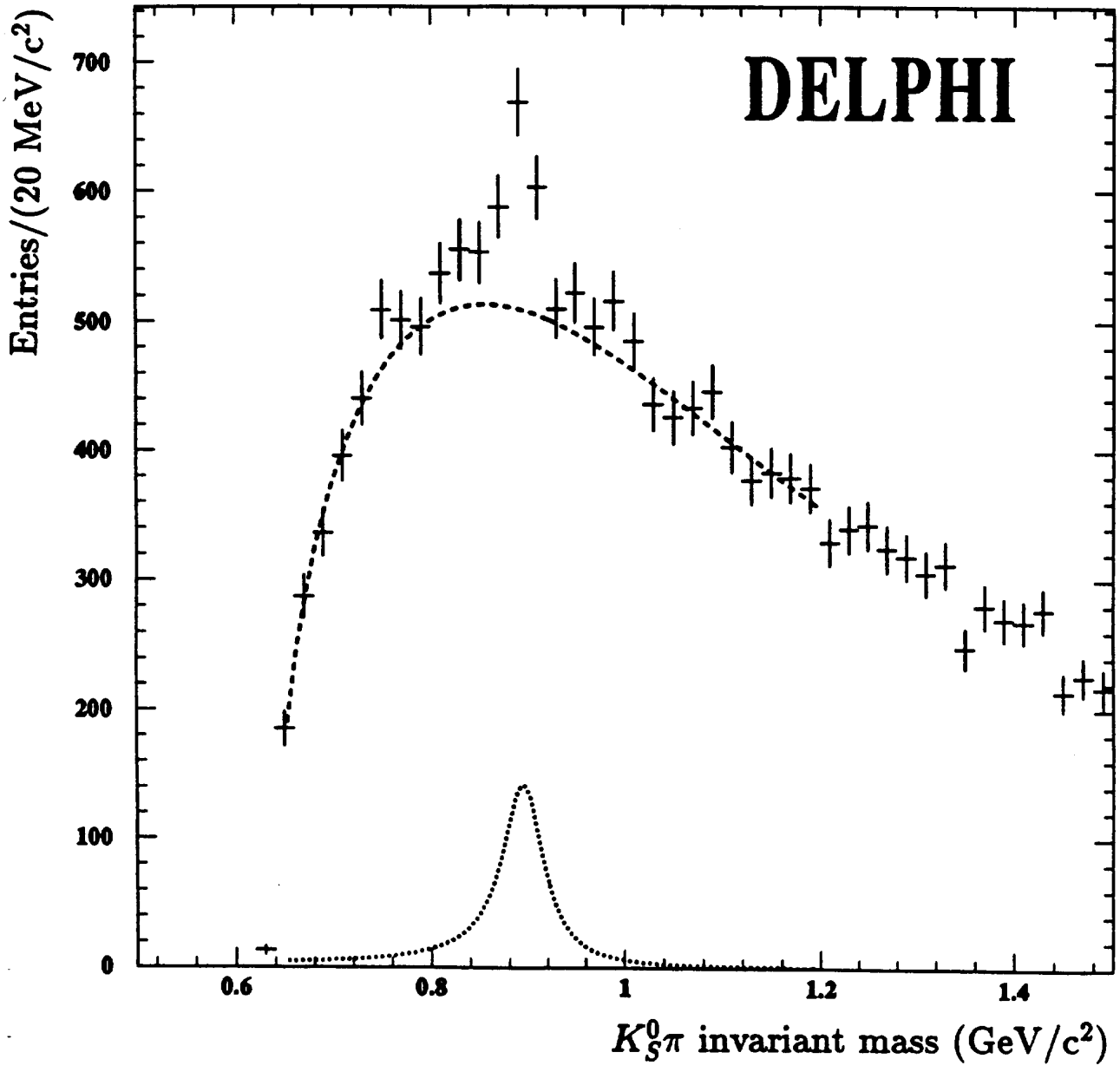
DELPHI
Entries/(20 MeV/c²)
700
600
500
400
300
200
100
0
0.6
0.8
1
1.2
1.4
$K^0_S\pi$ invariant mass (GeV/c²)

Figure 5

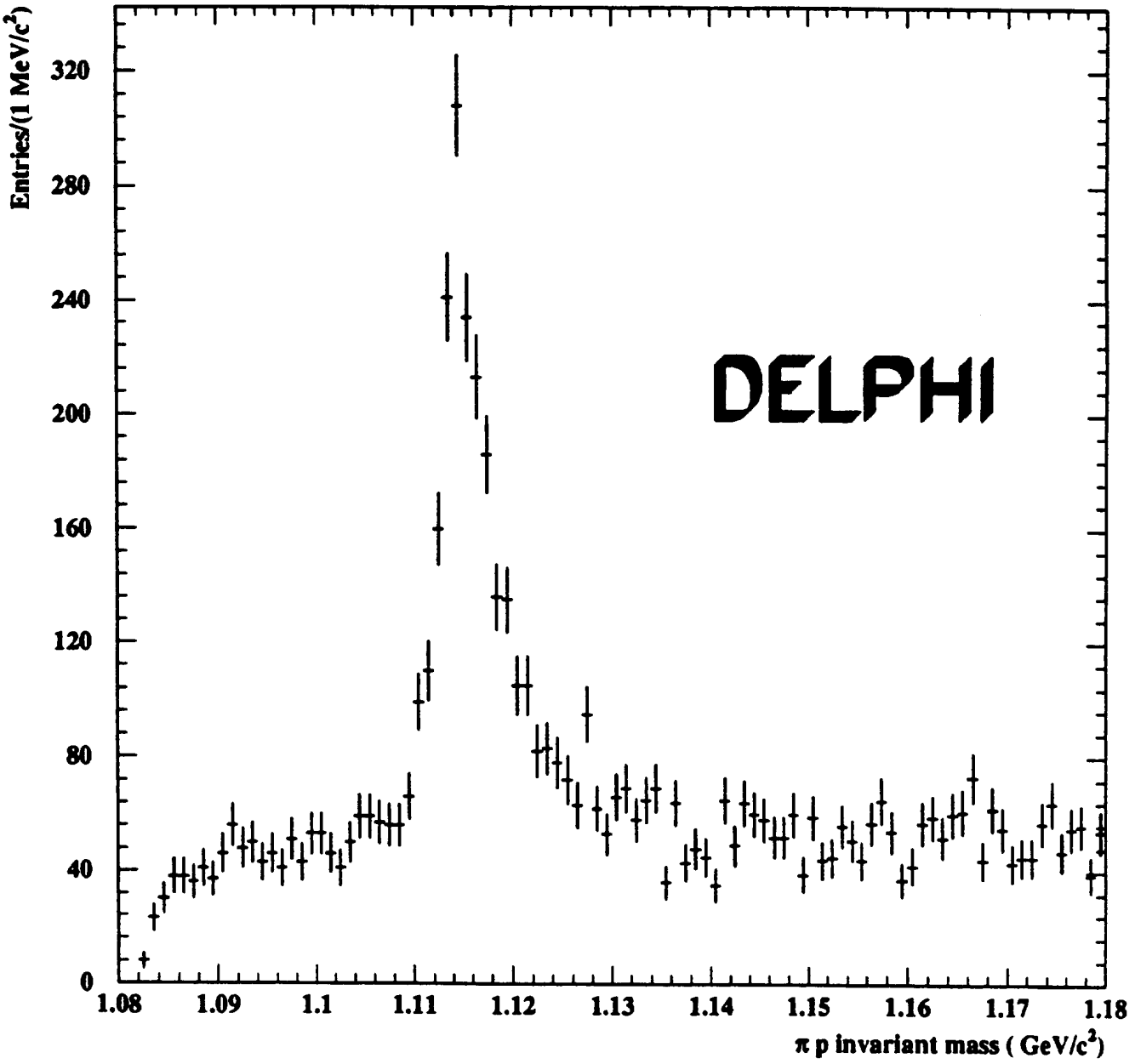
Entries/(1 MeV/c²)
320
280
240
200
160
120
80
40
0
1.08
1.09
1.1
1.11
1.12
1.13
1.14
1.15
1.16
1.17
1.18
π p invariant mass (GeV/c²)
DELPHI

Figure 6

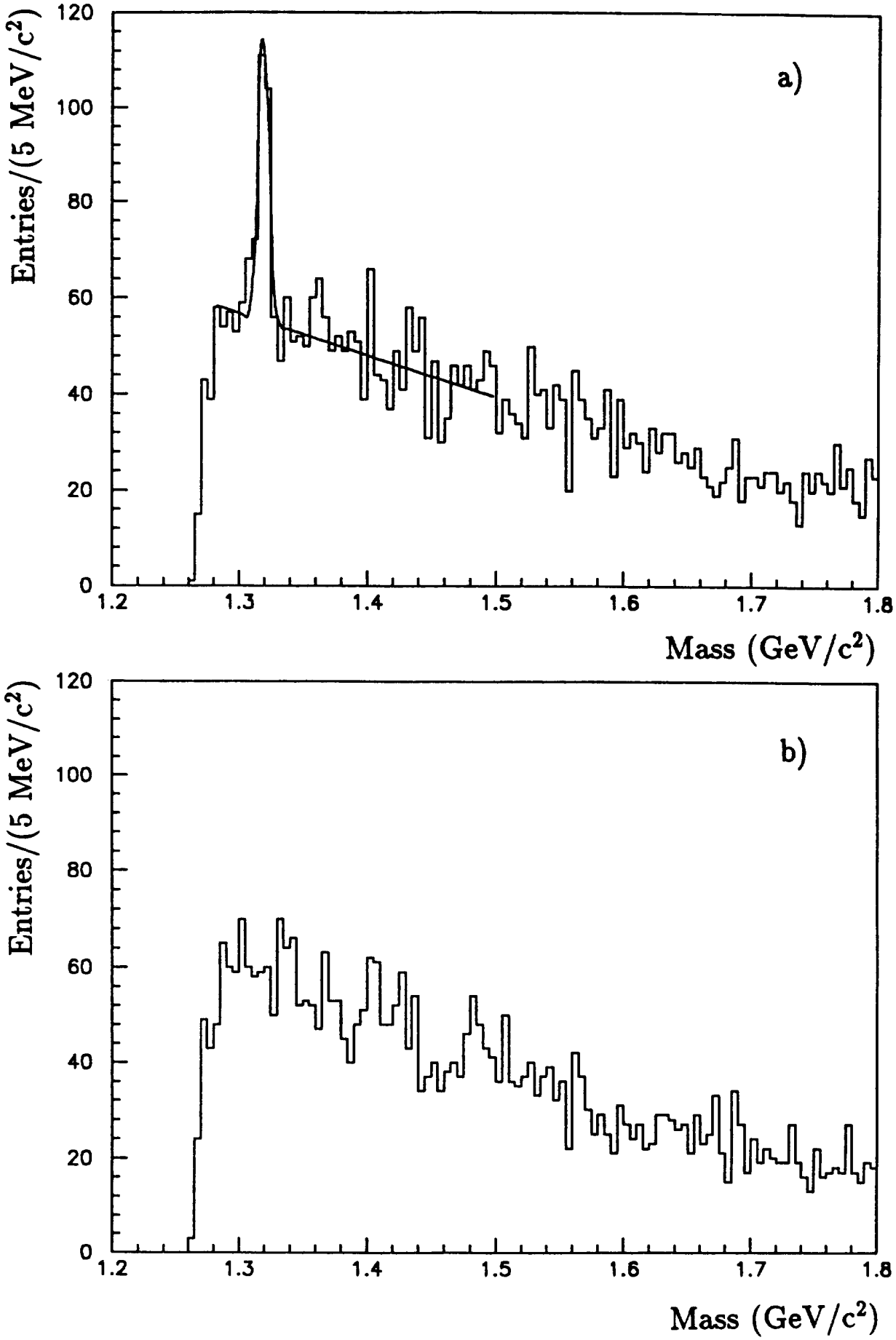
a)
b)
Entries/(5 MeV/c²)
Mass (GeV/c²)
0
20
40
60
80
100
120
1.2
1.3
1.4
1.5
1.6
1.7
1.8

Figure 7

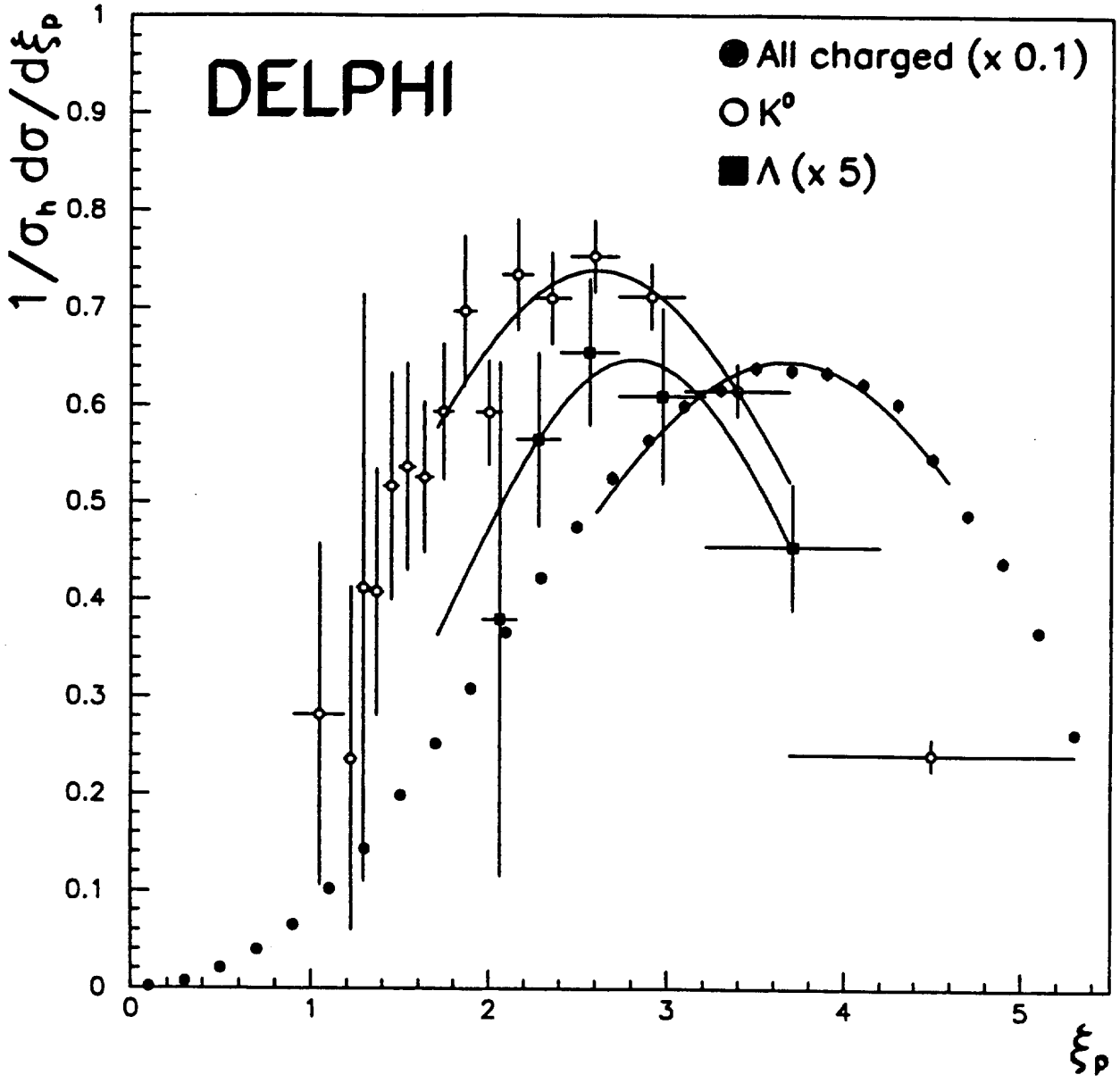

Imprimé au CERN. Prix : 0.65 Fr.